Applied Problems of Nonlinear Oscillation and Wave Theory

Izvestiya Vysshikh Uchebnykh Zavedeniy. Applied Nonlinear Dynamics. 2023;31(3)

Article DOI: 10.18500/0869-6632-003037

Coupled economic oscillations — synchronization dynamical model

V. V. Matrosov✉, *V. D. Shalfeev*

National Research Lobachevsky State University of Nizhny Novgorod, Russia
E-mail: ✉matrosov@rf.unn.ru, shalfeev@rf.unn.ru

Received 17.10.2022, accepted 15.12.2022, available online 14.04.2023, published 31.05.2023

Abstract. *Purpose* of this work is the research of the dynamical processes and in particular the phenomenon of the synchronization in an ensemble of coupled chaotic economic oscillators. *Methods.* The research methods are the qualitative and numerical methods of the theory of nonlinear dynamical systems and the theory of the bifurcations. *Results.* The nonlinear model of economic oscillator as the system of automatic control are considered. Such kind of general economic models are unsuitable for getting some concrete economic estimations and recommendations. But such kind models are very useful for a development the theory of the economic cycles, theory of the generation, interactions, synchronization of the cycles and so on. Our numerical experiments demonstrated a good enough qualitative similarity of an chaotic economic oscillations in our model and real economic cycles. The phenomen of the synchronization of the chaotic oscillations in the ensemble of coupled economic oscillators are considered, however the accuracy of the synchronization depends with couplings essentially.

Keywords: economic oscillation, dynamical chaos, synchronization.

Acknowledgements. This work was supported by the Ministry of Science and Higher Education of the Russian Federation (project No. FSWR-2023-0031). Authors are grateful to M. I. Rabinovich and V. P. Ponomarenko for useful discussions and tips.

For citation: Matrosov VV, Shalfeev VD. Coupled economic oscillations — synchronization dynamical model. Izvestiya VUZ. Applied Nonlinear Dynamics. 2023;31(3):254–270. DOI: 10.18500/0869-6632-003037

Introduction

Economic fluctuations (business cycles) have been the subject of close attention of economists for more than a decade. Despite the many theories put forward (the theory of periodic cycles, exogenous theories of the impact of natural disasters, social, technological shocks, endogenous theories of underconsumption, equilibrium cycle, over-accumulation, etc.) [1–4], it should be recognized that a single. There is no generally accepted theory of economic fluctuations today, as there is no single view on the causes that generate cycles [5]. The question of synchronizing economic fluctuations is even more unclear and confusing. A number of authors study the synchronization of cycles based on the analysis of time-series [6]. However, in most economic

works, synchronization is understood not as a coincidence of oscillation frequencies, but as some proximity concordance analysis, based on the proximity of «phases» (stages) of cycles [7]. There are authors — supporters of the application of the theory of dynamic chaos in economics and finance, in particular for the analysis of synchronization [8, 9].

In [10, 11], a dynamic model of a chaotic economic oscillator functioning as an automatic control system and the processes of generating and synchronizing economic cycles based on this model are considered. The present work is a development of these studies, in particular, continues the study of synchronization processes in an ensemble of related economic oscillators.

The work is organized as follows. Section 1 discusses the dynamic model of the economic oscillator. Section 2 presents the results of a study of synchronization processes in an ensemble of coupled oscillators.

1. Model of economic fluctuations

In [10, 11], the idea of constructing a nonlinear model of a hypothetical economic oscillator functioning as a typical automatic control system is considered. This approach to describing the dynamic behavior of various technical, biological, social, and other objects is not new. In the literature, you can find many examples of using this approach, in particular, an example of building a dynamic buyer model in the task of forming public opinion [12].

How can we build a model of an economic oscillator using the ideas of the theory of automatic control? Economic fluctuations (business cycles) are determined by several indicators, among which the most important is the gross domestic product (GDP), characterized by the total amount of goods and services produced in the country. Let's choose one specific type of product from the composition of GDP and build a chain of automatic control, where as an input signal we will take the trend value of the value of this product (constant or changing over time), and as an object of control we will take a certain appraiser of the value of the product. The control circuit will adjust the evaluator's output signal according to the input signal. The functions of the various elements of the control chain of the constructed hypothetical system, obviously, should be implemented by the managers actions of the government of the country, investment banks, management of enterprises, etc., etc. Since the selected product is produced, as a rule, not by one manufacturer, but by several, it may be necessary to organize a multi-circuit management system. The presence of many agents involved in management may result in inconsistency of control actions. The unavoidable presence of inertia and delays in control circuits can lead to instabilities that generate the appearance of limit cycles and chaotic attractors, as a result of which periodic and chaotic oscillations will form at the output of the system. To estimate the value of the cost of other goods and services that make up the GDP, other management systems should be built in the same way. Summing up the output signals of all the built control systems will allow us to get an estimate of the value of GDP and its dynamics, that is, to get a business cycle model as a result. It is obvious that the model obtained as a result of such constructions, which includes a large number of multi-circuit control systems, will be so cumbersome, this will not allow conducting a dynamics study and obtaining any specific data about the business cycle, since most of the parameters of the constructed model will be unknown. Taking into account this circumstance, it seems more expedient to implement the simplest version of an automatic control system for evaluating only one indicator - the composite business cycle index.

The model of an economic oscillator functioning as an automatic control system for the value of the composite business cycle index [10, 11] is shown in Fig. 1.

Here the object of control is the estimator E, the output of which generates the current estimate of the value of the composite index of the business cycle $I_{\mathsf{E}}(t)$. The input of the system receives $I_{\mathsf{R}}(t)$ — the value of the real business cycle index determined by the real sector of the

economy (for simplicity, let's put it constant). The discriminator $I_{\mathsf{E}}(t)$ and $I_{\mathsf{R}}(t)$. The signal from the output of D passes through the filter F, removes high-frequency noise. The signal from the output of the filter U_{F} goes to the controller C, which corrects the estimate of $I_{\mathsf{E}}(t)$ by the amount of Δ_I in the direction of rapprochement with $I_{\mathsf{R}}(t)$.

The equation describing the dynamics of the economic oscillator model (see Fig. 1), obtained in [10, 11] in operator form:

$$x + K(p)\Phi(x) = \gamma, \quad p \equiv d/dt. \tag{1}$$

Here $x = (I_{\mathsf{E}} - I_{\mathsf{R}})/\Delta I_{\max}$ — the dimensionless current deviation of the I_{E} value of the composite business cycle index from the value of I_{R} of the real composite index of the business cycle. $\Delta I_{\max} = SE$ (S — steepness of the controller characteristic, E — maximum value of the output signal D), $\gamma = (I_{\mathsf{E}}^0 - I_{\mathsf{R}})/\Delta I_{\max}$ — dimensionless deviation of the value of the composite index of the business cycle I_{E}^0 at the initial time from the values of I_{R} of the real composite index of the business cycle, $K(p)$ — the transfer function of the filter, $\Phi(x)$ — the nonlinearity of the discriminator D, normalized to one.

Taking $K(p) = (1 + a_1 p + a_2 p^2 + a_3 p^3)^{-1}$ and introducing dimensionless time $\tau = t/a_1$ and parameters $\varepsilon = a_2/a_1^2$, $\mu = a_3/a_1^3$, write the equation (1) as

$$\begin{aligned} \frac{dx}{d\tau} &= y, \quad \frac{dy}{d\tau} = z, \\ \mu\frac{dz}{d\tau} &= \gamma - x - y - \varepsilon z - \Phi(x). \end{aligned} \tag{2}$$

Dynamics (2) has been studied in a number of papers, in particular, in [13] for $\Phi(x) = 2\beta x/(1 + \beta^2 x^2)$ at $\beta > 0$, in [14] for inverted nonlinearity $\Phi(x)$ at $\beta < 0$, as well as in [15], etc. Here is a brief overview of the dynamics (2).

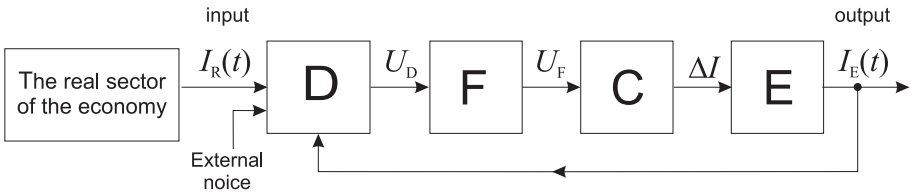

Fig. 1. The model of economic oscillator: E — estimator, C — control element, F — filter, D — discriminator

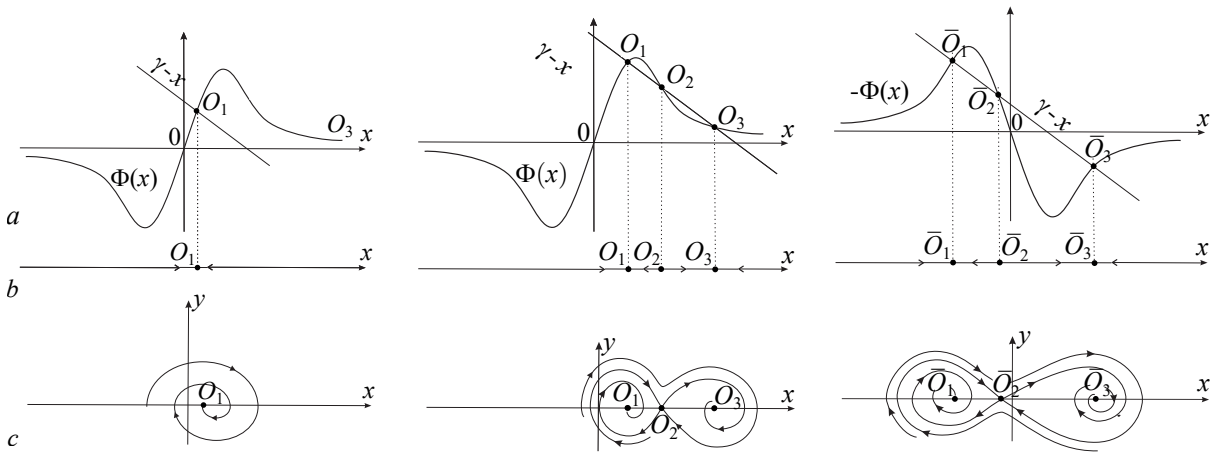

Fig. 2. Equilibrium states of the system (2) (a), phase portraits of the system (2) when $\mu = 0$, $\varepsilon = 0$ (b), phase portraits of the system (2) when $\mu = 0$, $\varepsilon \neq 0$ (c)

For $\mu = 0$, $\varepsilon = 0$, the system (2) reduces to a first-order equation, and for $\mu = 0$, $\varepsilon \neq 0$ — to a second-order equation. The dynamics (2) in these cases is determined by the equilibrium states (Fig. 2, *a*). For non-inverted nonlinearity $\Phi(x)$, there is one stable equilibrium state $O_1(O_3)$, or three — O_1, O_3 — stable and O_2— unstable, and for inverted nonlinearity $\Phi(x)$ one stable equilibrium state $\bar{O}_1$ ($\bar{O}_3$), or three — $\bar{O}_1$ ($\bar{O}_3$) — stable and $\bar{O}_2$ — unstable. In Fig. 2, *b* the characteristic phase portraits of the system (2) are given for $\mu = 0$, $\varepsilon = 0$, and in Fig. 2, *c* — phase portraits for $\mu = 0$, $\varepsilon \neq 0$ obtained by standard methods of oscillation theory [16].

The dynamics of the system (2) in the three-dimensional phase space (x, y, z) is quite complex and is characterized not only by the presence of equilibrium states, but also by the presence of limit cycles and chaotic attractors, as about one equilibrium state O_1 or O_3 ($\bar{O}_1$ or $\bar{O}_3$), and about three equilibrium states O_1, O_2, O_3 ($\bar{O}_1$, $\bar{O}_2$, $\bar{O}_3$).

Without giving here a complete description of the dynamics (2), we present the most important bifurcations from the point of view of economic interpretations, illustrating different ways of excitation of chaotic oscillations in the system (2).

For the case of the non-inverted characteristic $\Phi(x)$ in Fig. 3 presents a parametric portrait (μ, γ) of the system (2) for $\varepsilon = 1$, $\beta = 10$.

Here the dashpoint line $\gamma = \gamma^*$ corresponds to the bifurcation of the fusion of the equilibrium states O_2 and O_3, and the dashpoint line $\gamma = \gamma^{**}$ corresponds to the bifurcation of the fusion of equilibrium states O_2 and O_1. The lines $\gamma = \gamma^*$ and $\gamma = \gamma^{**}$ limit the region C_1 of the existence of the equilibrium state O_1, the region C_2 of the existence of the equilibrium states O_1, O_2, O_3 and the region C_3 the existence of a state of equilibrium O_3.

Line 1 corresponds to the Andronov–Hopf bifurcation for the equilibrium state O_1. The first Lyapunov quantity on *lines 1* is negative, hence this bifurcation is supercritical and *line 1* corresponds to the soft birth of a stable limit cycle L_1 around O_1 (fig. 4, *a*) when crossing *lines 1* from left to right.

Dotted *lines 2* and *3* correspond to the first period doubling bifurcation of the cycle L_1, after which the cycle L_1 undergoes a series of period doubling bifurcations, resulting in a chaotic

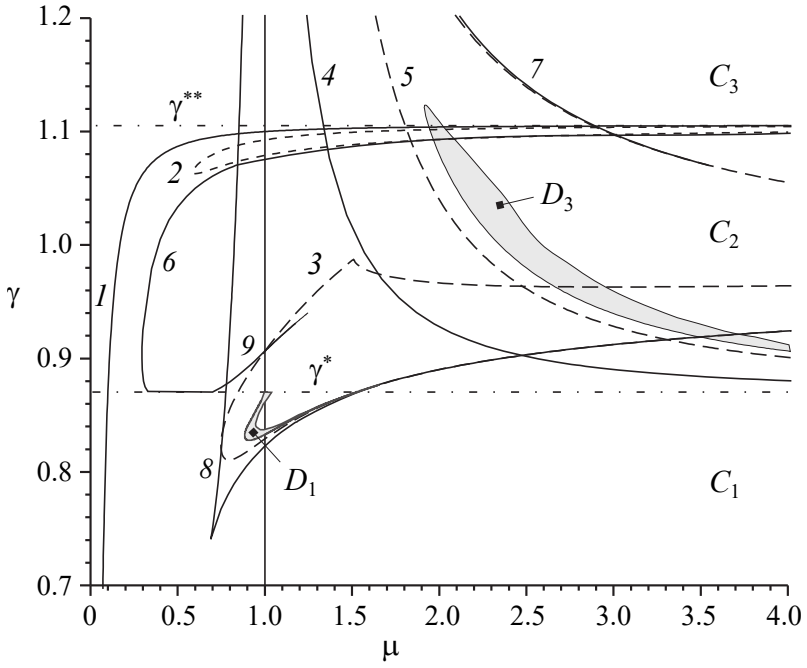

Fig. 3. Parametric portrait of the (2) when $\varepsilon = 1$, $\beta = 10$

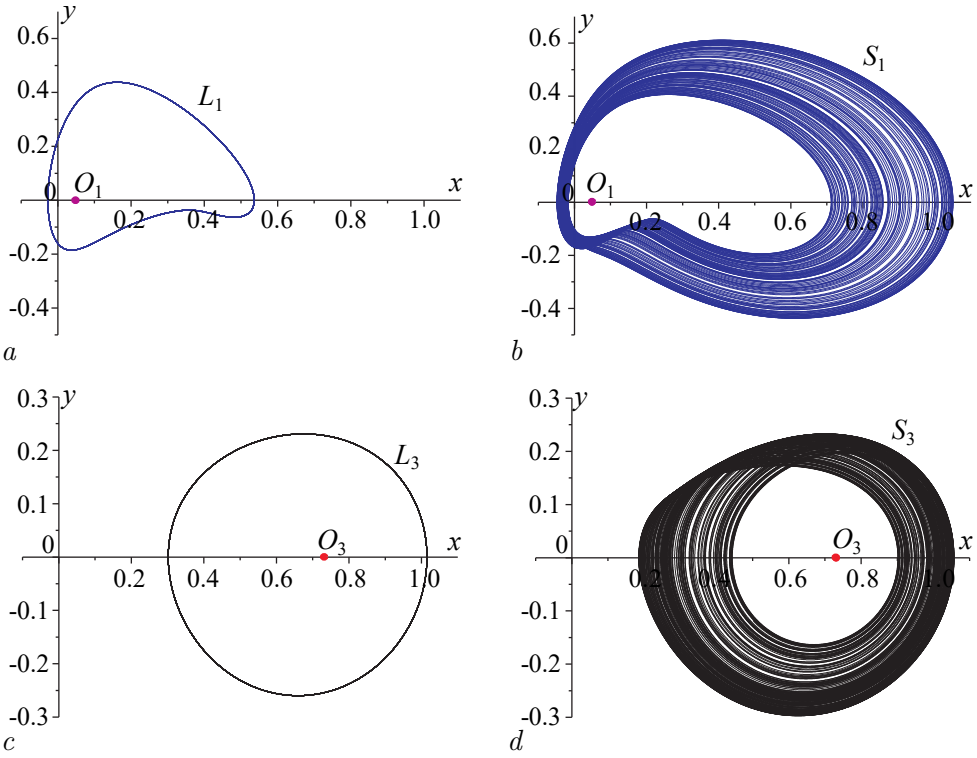

Fig. 4. Projections of attractors of (2) when $\varepsilon = 1$, $\beta = 10$, $\gamma = 0.835$, $\mu = 0.4$ (a), $\gamma = 0.835$, $\mu = 0.9$ (b), $\gamma = 1$, $\mu = 2.1$ (c), $\gamma = 1$, $\mu = 0.239$ (d) (color online)

attractor S_1 appears in accordance with Feigenbaum's scenario (Fig. 4, b).The area of existence of the attractor S_1, bounded by *line 2*, is very small and therefore in Fig. 3 is not shown, and the region of existence of the attractor S_1, bounded by *line 3*, is indicated by D_1 in Fig. 3.

Line 4 corresponds to the loss of stability of the equilibrium state O_3 as a result of the Andronov–Hopf bifurcation. The first Lyapunov quantity on *line 4* is negative, that is, it is a supercritical bifurcation and on *line 4* a stable limit cycle L_3 is gently born around O_3 (Fig. 4, c).

The dotted *line 5* corresponds to the first bifurcation of doubling the period of the cycle L_3, then through a series of bifurcations of doubling the period, a chaotic attractor S_3 is born in accordance with the scenario Feigenbaum (fig. 4, d). The domain of existence of the attractor S_3 is denoted by D_3 in fig. 3.

In addition to the bifurcations described above, the system (2) demonstrates other bifurcations, in particular, the bifurcation of the L_1 cycle sticking into the saddle separatrix loop O_2 followed by the disappearance of L_1 (*line 6*), saddle-node bifurcation of the disappearance of the L_3 cycle (*line 7*), saddle-node bifurcation of the birth of the cycle L_2, covering all three equilibrium states O_1, O_2, O_3 (*line 8*), loop bifurcation saddle-focus separatrix O_2 with negative saddle magnitude and positive saddle magnitude (*line 9*). In the latter case, there is a complex parametric portrait structure associated with an infinite number of bifurcation lines corresponding to multiple cycles and multi-pass loops of separatrix [17]. The analysis of these bifurcations is not given here, because it goes beyond the main purpose of the work.

Let us now turn to the dynamics of the system (2) in the case of inverted nonlinearity $\Phi(x)$. In Fig. 5 for this case, the most important bifurcation curves are presented, reflecting the occurrence and randomization of self-oscillatory modes in the model (2), and in Fig. 6 examples of projections corresponding to these modes of attractors are given.

The dotted line $\gamma = \gamma^*$ divides the plane of the parameters (μ, γ) into the regions C_1 and

C_2 of the existence of three ($\bar{O}_1$, $\bar{O}_2$, $\bar{O}_3$) and one ($\bar{O}_3$) equilibrium state.

Lines 1 and *2* (see fig. 5) are responsible for the birth of a stable limit cycle L_1 around the equilibrium state $\bar{O}_1$ (Fig. 6, *a*). *The line 1* corresponds to the Andronov–Hopf bifurcation of the equilibrium state $\bar{O}_1$. The point M, where the first Lyapunov quantity turns to zero, divides the bifurcation curve into sections of soft and hard excitation of self-oscillations. The part of *lines 1* located above the point M, corresponds to the supercritical Andronov-Hopf bifurcation, at the intersection of this section of the curve from left to right, the change in stability of the equilibrium state $\bar{O}_1$ is accompanied by the birth of a stable limit cycle L_1 of almost zero amplitude. The part of *lines 1* located below the point M corresponds to the hard birth of self-oscillations. A rigid self-oscillating mode occurs as a result of the bifurcation of a two-fold limit cycle on *lines 2*. *The line 2* is located below the point M and runs to the left of *lines 1*. When *lines 2* intersect from left to right in the phase space of the model (2), a stable limit cycle L_1 of finite amplitude appears.

The cycle L_1 may experience period doubling bifurcations, as a result of which a chaotic attractor S_1 may form on its basis (Fig. 6, *b*). The dotted *line 3* is responsible for the first bifurcation of doubling the period of the cycle L_1, this bifurcation is soft, and corresponds to the appearance of a stable limit cycle $L_1^{(2)}$ of the doubled period. Note that the process of doubling the cycle period L_1 does not always end with the formation of of a chaotic attractor, the Feigenbaum scenario can be interrupted by the disappearance of limit cycles of large periods either through tangent bifurcation or as a result of bifurcations of multi-pass loops of saddle separatries $\bar{O}_2$. In particular, in Fig. 5 solid *line 5* corresponds to the tangent bifurcation of the cycle $L_1^{(2)}$ of the doubled period, and the solid *line 6* — bifurcations of the two-way loop of the saddle-focus separatrix $\bar{O}_2$. *The line 4* bounds the area of existence of the cycle L_1 on the right, on this curve the cycle L_1 disappears through a tangent bifurcation. The regions of existence of the chaotic attractor S_1 on Fig. 5 are not highlighted because they have insignificant dimensions, however, dotted lines reflecting the transition from regular to chaotic oscillations are applied to the parametric portrait.

The line 7 is responsible for the birth of a stable limit cycle L_3 (Fig. 6, *c*) through the bifurcation of a two-fold limit cycle. At small γ at the moment of birth, the cycle L_3 covers the

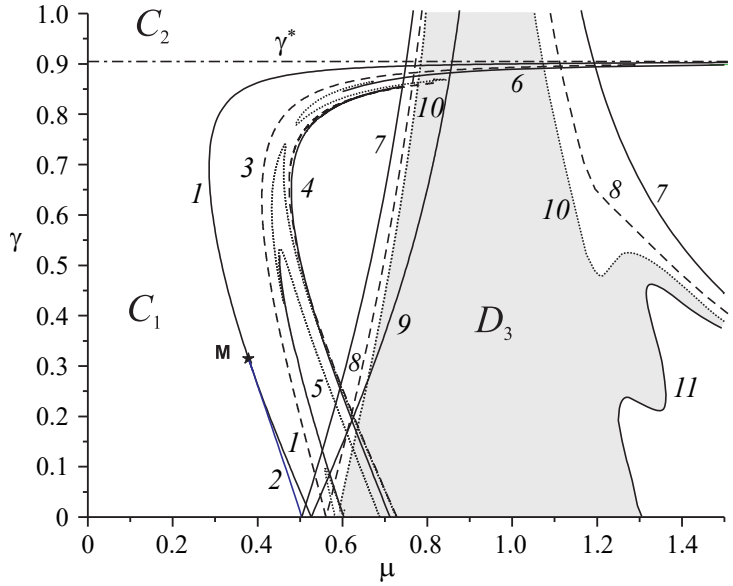

Fig. 5. Parameter portrait of the (2) when $\varepsilon = 1$, $\beta = -10$

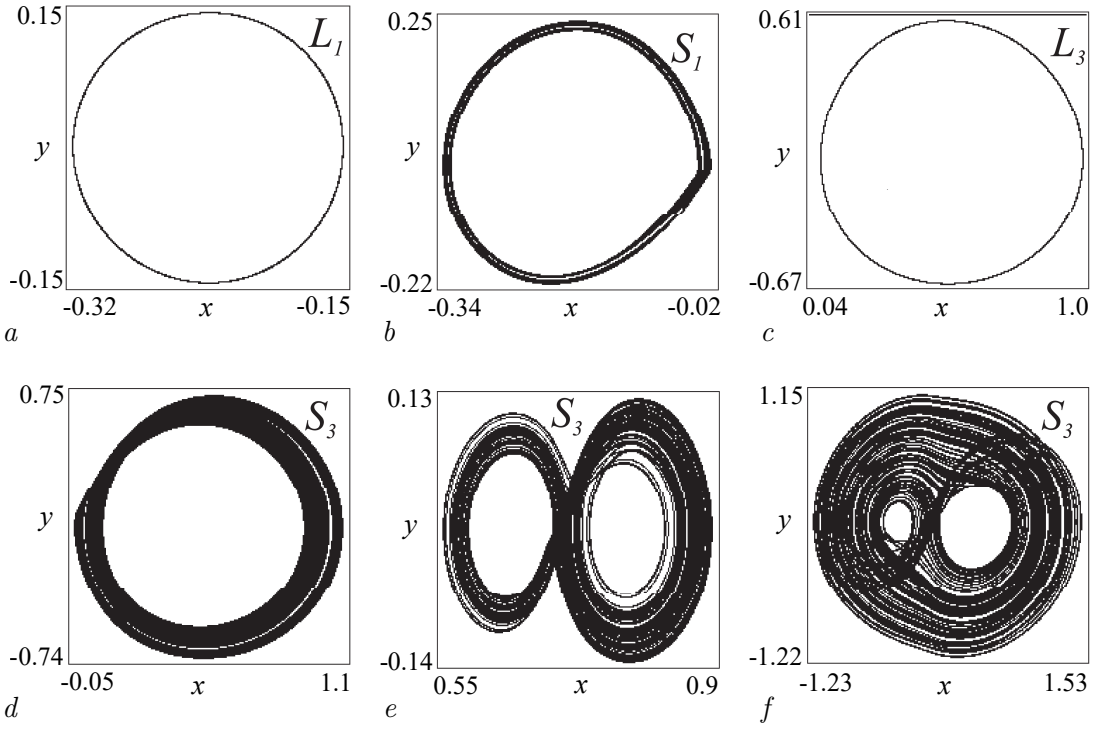

Fig. 6. Projections of attractors of the system (2) when $\varepsilon = 1$, $\beta = -10$, $\gamma = 0.5$, $\mu = 0.321$ (*a*), $\gamma = 0.6$, $\mu = 0.463$ (*b*), $\gamma = 0.05$, $\mu = 0.529$ (*c*), $\gamma = 0.1$, $\mu = 0.623$ (*d*), $\gamma = 0.1$, $\mu = 0.66$ (*e*), $\gamma = 0.1$, $\mu = 1.27$ (*f*)

equilibrium state $\bar{O}_3$, with the growth of γ, as well as with distance from *line 7*, the amplitude of the cycle L_3 grows, and it begins to cover all three equilibrium states.

The dotted *line 8* corresponds to the beginning of the doubling of the period of the cycle L_3, when moving away from this line, the cycle L_3 experiences a cascade of bifurcations of doubling of the period, as a result, a chaotic attractor is formed on the basis of L_3 S_3 (Fig. 6, *d*). *The lines 9* and *11* limit the region D_3 of the existence of chaotic oscillations. The dot *line 10* reflects the fourth bifurcation of doubling the period of the cycle L_3, and since the bifurcation values of the fifth and subsequent bifurcations of doubling the period L_3 fit into the interval $\Delta\mu = 10^{-4}$, the value of the fourth bifurcation of doubling the period can practically be used in as the boundary of the region of existence of chaotic oscillations. On the solid *line 11*, a chaotic attractor crisis occurs, when leaving the D_3 region through this line, the S_3 attractor collapses, phase trajectories from its vicinity rush to infinity. Note that chaotic oscillations of S_3 can take a different form, this indicates the wide possibilities of the model under consideration for generating chaotic oscillations with different characteristics. Examples of possible projections of the attractor S_3 are shown in Fig. 6, *d–f*.

Thus, the above data show that the model (2) demonstrates extensive possibilities for generating chaotic modes. Comparison of oscillograms of such chaotic oscillations [10,11] with the oscillograms of real fluctuations of composite business cycle indices, given in the literature [18], makes it possible to conclude that there is a fairly good qualitative similarity of such fluctuations.

2. Analysis of synchronization processes of related economic fluctuations

Let's consider the dynamics of a small ensemble of five economic oscillators (2) connected according to the scheme of Fig. 7.

Connections according to the scheme Fig. 7 allow us to investigate synchronization processes in the ensemble depending on the strength of the connections with the oscillator O_0. We will consider the connections of the oscillators O_1, O_2, O_3, O_4 are approximately the same, and the connections from the O_0 oscillator will vary from weak to strong. Such a situation can simulate the processes of economic interaction between a group of countries with approximately the same economy and one country with a significantly stronger economy.

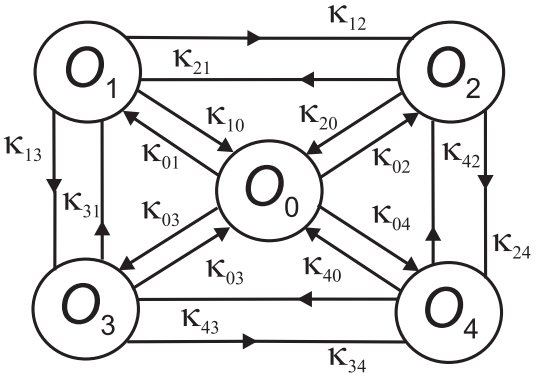

Fig. 7. The ensemble of oscillators

The system of equations describing the dynamics of the ensemble shown in Fig. 7, can be written as

$$
\begin{aligned}
\frac{dx_1}{d\tau} &= y_1, \quad \frac{dy_1}{d\tau} = z_1,\\
\mu_1\frac{dz_1}{d\tau} &= \gamma_1 - x_1 - y_1 - \varepsilon_1 z_1 - \Phi_1(x_1) - \kappa_{21}\Phi_2(x_2) - \kappa_{31}\Phi_3(x_3) - \kappa_{01}\Phi_0(x_0),\\
\frac{dx_2}{d\tau} &= y_2, \quad \frac{dy_2}{d\tau} = z_2,\\
\mu_2\frac{dz_2}{d\tau} &= \gamma_2 - x_2 - y_2 - \varepsilon_2 z_2 - \Phi_2(x_2) - \kappa_{12}\Phi_1(x_1) - \kappa_{42}\Phi_4(x_4) - \kappa_{02}\Phi_0(x_0),\\
\frac{dx_3}{d\tau} &= y_3, \quad \frac{dy_3}{d\tau} = z_3,\\
\mu_3\frac{dz_3}{d\tau} &= \gamma_3 - x_3 - y_3 - \varepsilon_3 z_3 - \Phi_3(x_3) - \kappa_{13}\Phi_1(x_1) - \kappa_{43}\Phi_4(x_4) - \kappa_{03}\Phi_0(x_0),\\
\frac{dx_4}{d\tau} &= y_4, \quad \frac{dy_4}{d\tau} = z_4,\\
\mu_4\frac{dz_4}{d\tau} &= \gamma_4 - x_4 - y_4 - \varepsilon_4 z_4 - \Phi_4(x_4) - \kappa_{24}\Phi_2(x_2) - \kappa_{34}\Phi_3(x_3) - \kappa_{04}\Phi_0(x_0),\\
\frac{dx_0}{d\tau} &= y_0, \quad \frac{dy_0}{d\tau} = z_0,\\
\mu_0\frac{dz_0}{d\tau} &= \gamma_0 - x_0 - y_0 - \varepsilon_0 z_0 - \Phi_0(x_0) - \kappa_{10}\Phi_1(x_1) - \kappa_{20}\Phi_2(x_2) - \kappa_{30}\Phi_3(x_3) - \kappa_{40}\Phi_4(x_4).
\end{aligned}
\tag{3}
$$

In Fig. 8–10 the results of numerical experiments with the system are presented (3). Projections of chaotic attractors for the case of the absence of connections with the oscillator O_0 are given in Fig. 8. In this case, the oscillators O_1 — O_4 are synchronized, and there is no synchronization with the oscillator O_0. In Fig. 9 the case of weak connections with an oscillator is presented O_0. In this case, the synchronization of the oscillators O_1 — O_4 remained approximately at the same level, at the same time, there was a weak synchronization with the O_0 oscillator. In Fig. 10 the case of strong connections with the O_0 oscillator is presented, in this case the synchronization of O_1–O_4 has significantly improved and there is quite noticeable synchronization of O_0 with other oscillators.

As follows from Fig. 8–10, the accuracy of the obtained synchronization of chaotic oscillations

turned out to be low. It can be increased by strengthening the links, but even a triple increase in the strength of the links with the element O_0 (Fig. 10) did not lead to a significant increase in synchronization accuracy.

Next, let's consider the influence of connection parameters on the magnitude of synchronization errors. As a quantitative assessment of the synchronization accuracy of the i and j oscillators, we will use the value $\Delta_{i,j}$ calculated by the formula

$$\Delta_{i,j} = \max_{\tau\in[0,T]} |x_i(\tau) - x_j(\tau)| / \sqrt{(x_i^{\min} - x_j^{\min})^2 + (x_i^{\max} - x_j^{\max})^2}. \quad (4)$$

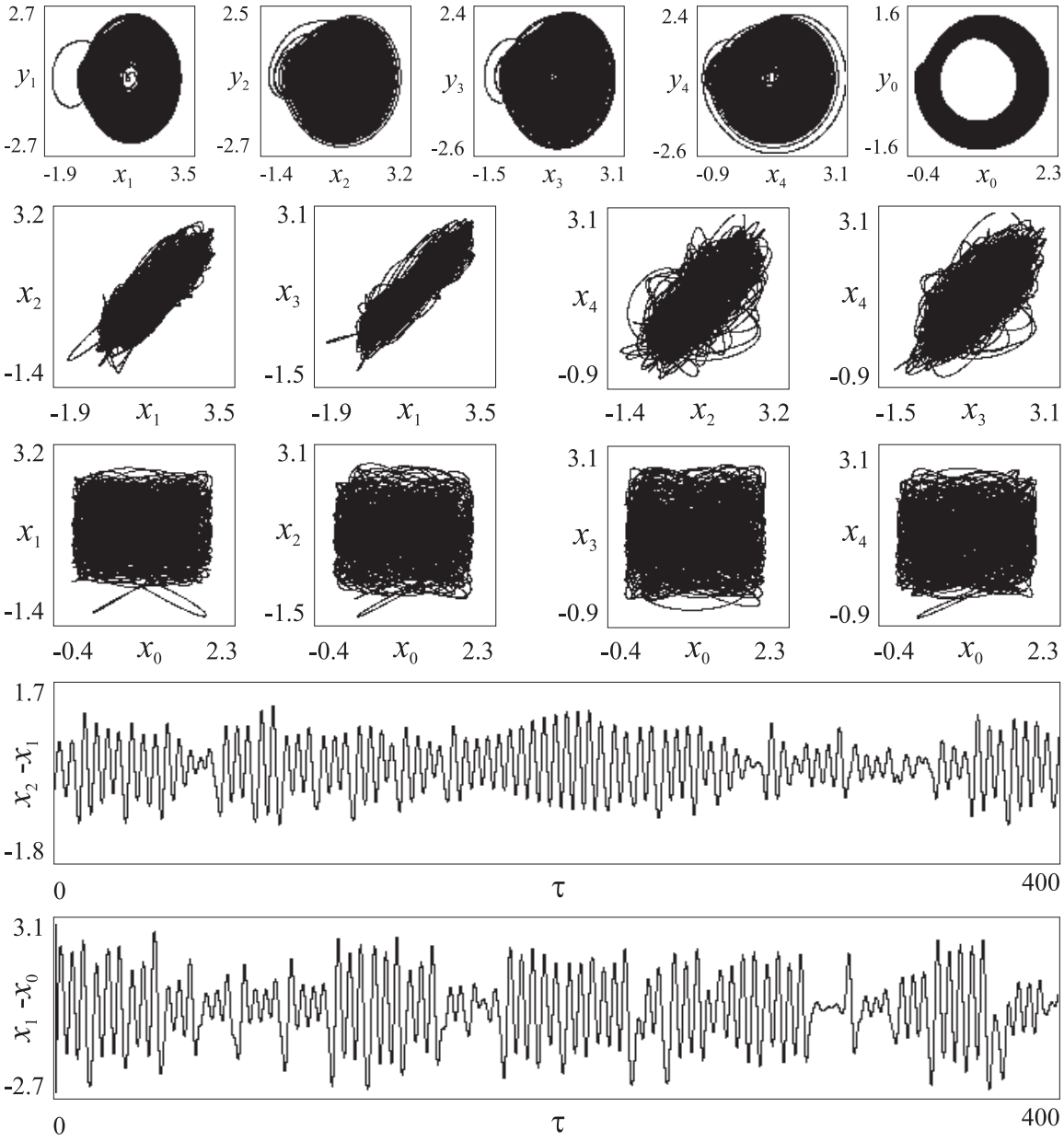

Fig. 8. Projections of attractors of the system (3) when couplings from oscillator O_0 are absent and $\gamma_0 = 0.64$, $\varepsilon_0 = 0.64$, $\mu_0 = 0.53$, $\beta_0 = -10$, $\gamma_1 = 0.64$, $\varepsilon_1 = 0.64$, $\mu_1 = 0.53$, $\beta_1 = -10$, $\gamma_2 = 0.65$, $\varepsilon_2 = 0.61$, $\mu_2 = 0.51$, $\beta_2 = -10$, $\gamma_3 = 0.64$, $\varepsilon_3 = 0.61$, $\mu_3 = 0.51$, $\beta_3 = -10$, $\gamma_4 = 0.63$, $\varepsilon_4 = 0.65$, $\mu_4 = 0.52$, $\beta_4 = -10$, $\kappa_{21} = 0.8$, $\kappa_{31} = 0.98$, $\kappa_{12} = 1$, $\kappa_{42} = 0.1$, $\kappa_{13} = 1$, $\kappa_{43} = 0.06$, $\kappa_{24} = 0.4$, $\kappa_{34} = 0.84$, $\kappa_{01} = \kappa_{02} = \kappa_{03} = \kappa_{04} = 0$, $\kappa_{10} = \kappa_{20} = \kappa_{30} = \kappa_{40} = 0$

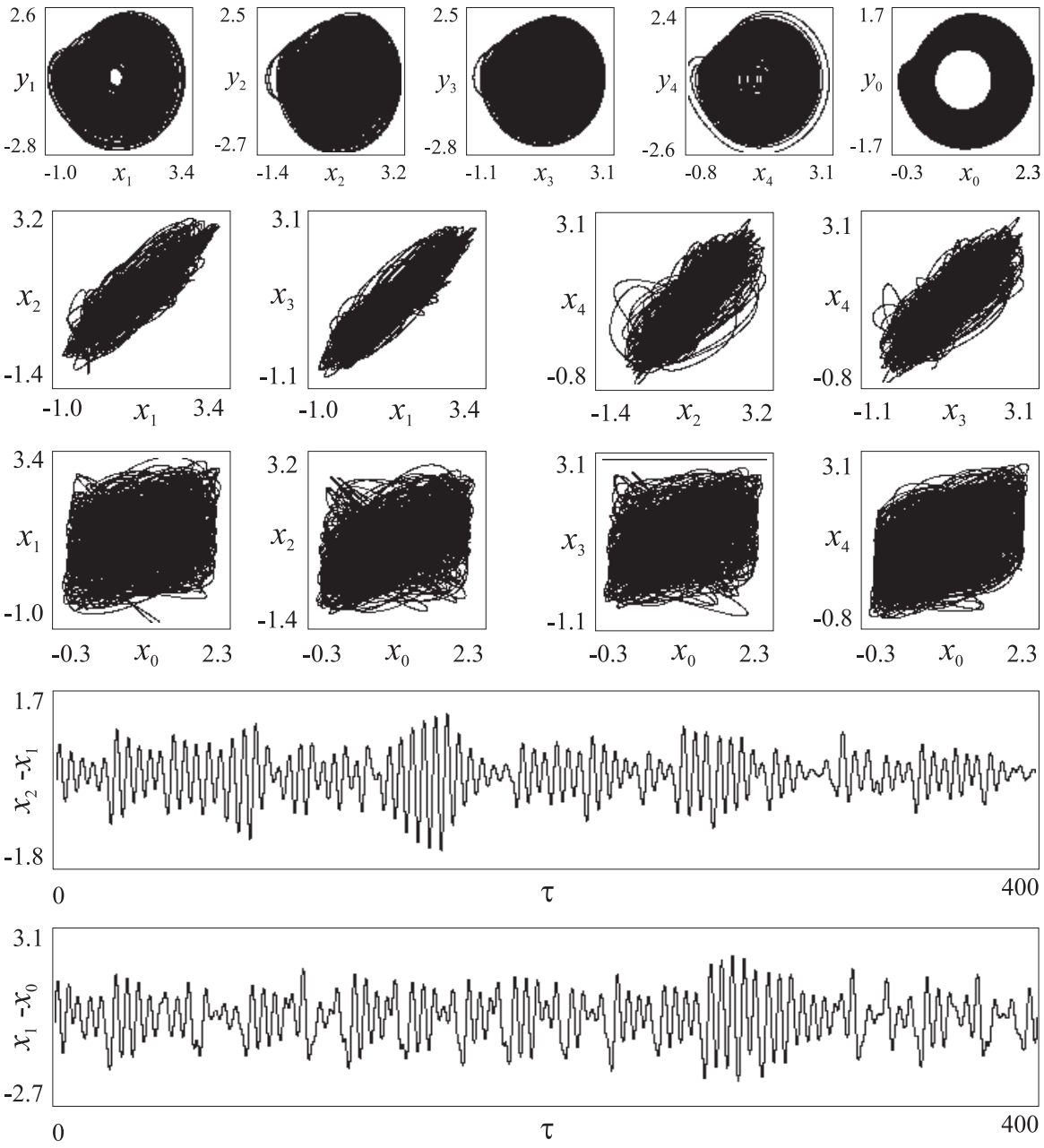

Fig. 9. Projections of attractors of the (3) when couplings from oscillator O_0 are weak and $\kappa_{01} = \kappa_{02} = \kappa_{03} = \kappa_{04} = 0.3$, $\kappa_{10} = \kappa_{20} = \kappa_{30} = \kappa_{40} = 0.05$

This value characterizes the maximum deviation of the phase variables $x_i(\tau)$ and $x_j(\tau)$ from the line $x_i = x_j$ during the observation time T, related to the size of the attractor projection on the plane of the corresponding coordinates [19]. Quantitative estimates of the synchronization accuracy of the ensemble oscillators, calculated by the formula (4) at the interval $T = 15,000$, are shown in Fig. 11. From the above results it follows that the dependence $\Delta_{i,j}$ from κ is an irregular process in general with a declining trend. Solid thick lines in Fig. 11 are the result of smoothing the values of $\Delta_{i,j}$ using the algorithm Savitsky–Goley, which more clearly reflect the trends in the evolution of synchronization errors with increasing connectivity. From the analysis of the

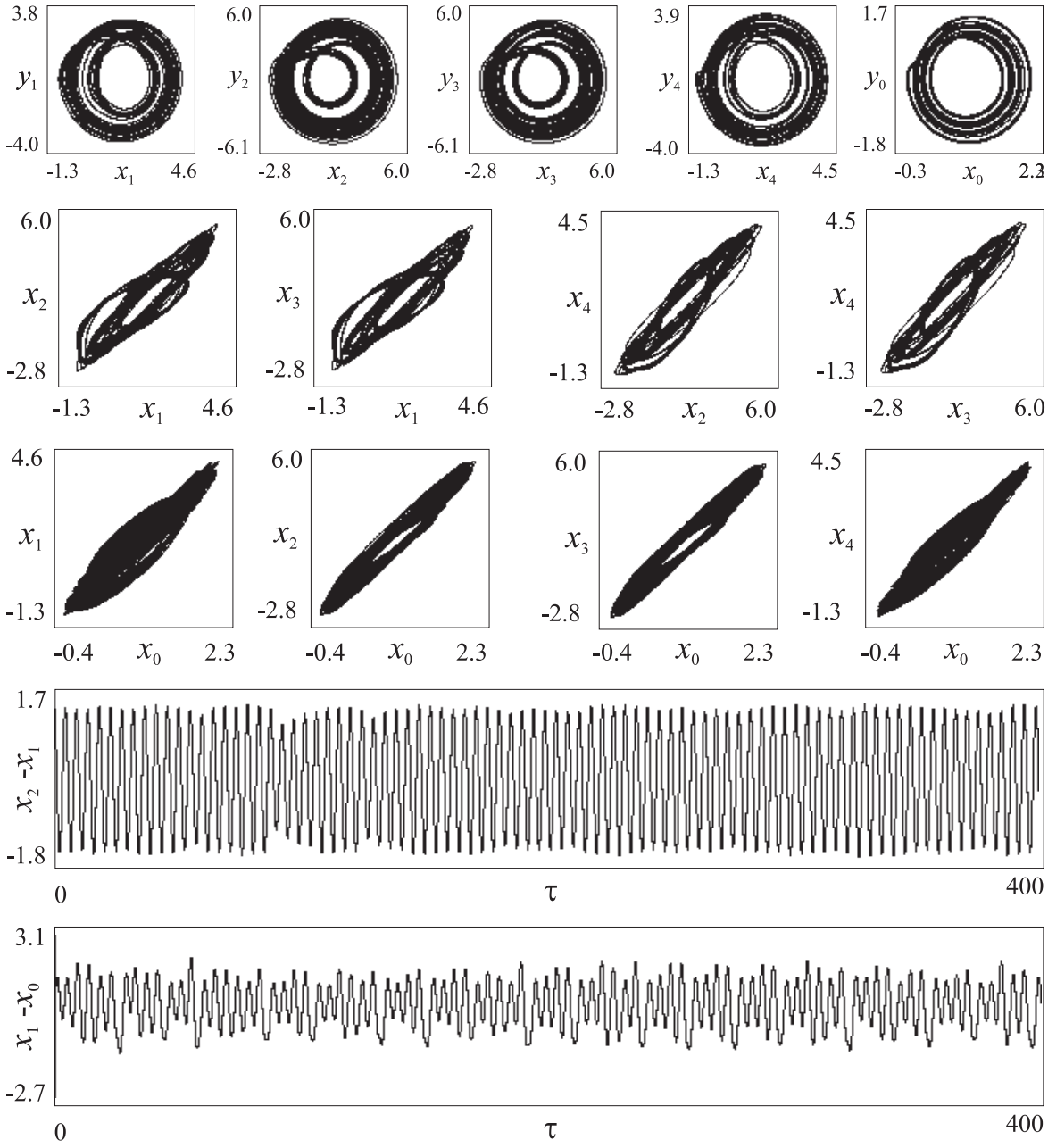

Fig. 10. Projections of attractors of the (3) when couplings from oscillator O_0 are strong and $\kappa_{01} = \kappa_{02} = \kappa_{03} = \kappa_{04} = 3$, $\kappa_{10} = \kappa_{20} = \kappa_{30} = \kappa_{40} = 0.1$

presented results, it follows that synchronization errors with the growth of κ do not decrease monotonously; $\Delta_{1,2}$ and $\Delta_{3,4}$ decrease; $\Delta_{1,0}$ and $\Delta_{3,0}$ have minima*. Note that the strengthening of the bonds entails an increase in the size of the attractor, and can also lead to the regularization of chaotic oscillations of oscillators. In in the latter case, there is a sharp decrease in the values of $\Delta_{i,j}$. In Fig. 11 sharp «dips» $\Delta_{i,j}$, in particular, in the area of κ =2.26 is due to the regularization of chaotic oscillations.

*The values of $\Delta_{1,3}$ and $\Delta_{2,4}$ are close to the values of $\Delta_{1,2}$ and $\Delta_{3,4}$, and the values of $\Delta_{2,0}$ and $\Delta_{4,0}$ — to the values of $\Delta_{1,0}$ and $\Delta_{3,0}$, respectively.

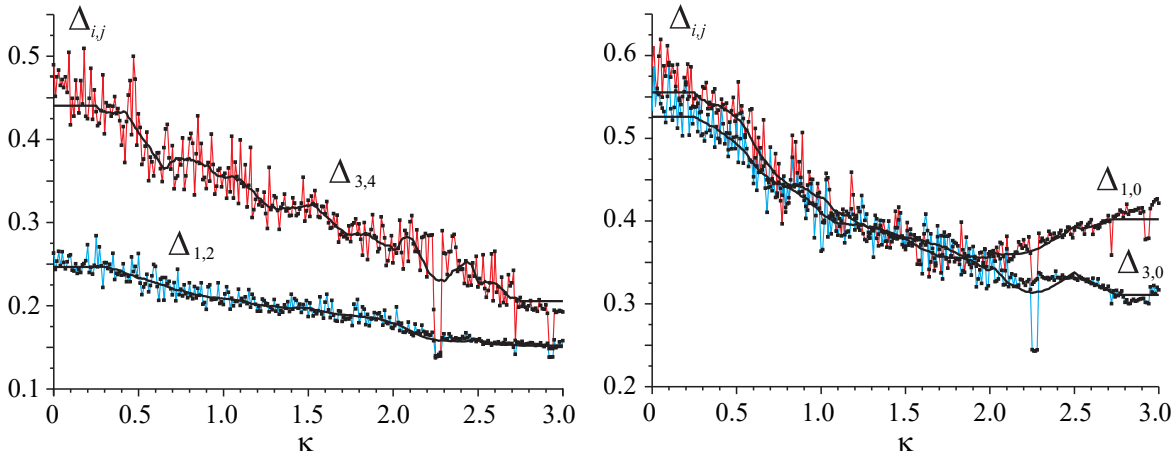

Fig. 11. The evolution of synchronization errors when couplings from oscillator O_0 are $\kappa_{01} = \kappa_{02} = \kappa_{03} = \kappa_{04} = \kappa$, $\kappa_{10} = \kappa_{20} = \kappa_{30} = \kappa_{40} = 0.1$ (color online)

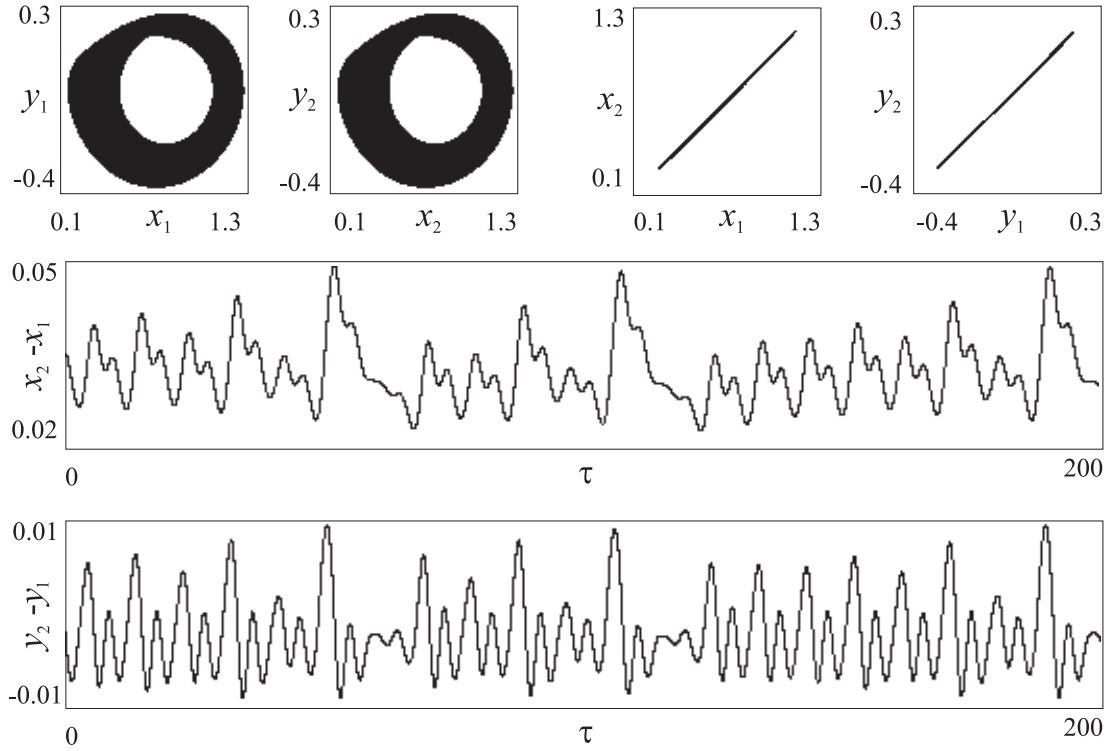

Fig. 12. Projections of attractors of the (5) when $\gamma_1 = 1.06$, $\varepsilon_1 = 1$, $\mu_1 = 2.1$, $\gamma_2 = 1.05$, $\varepsilon_2 = 0.96$, $\mu_2 = 2.06$, $\beta_1 = 10$, $\beta_2 = 10$, $\kappa_1 = 0.07$, $\kappa_2 = 0.2$

Another way to improve synchronization is to change the type of connections, namely, the organization of oscillator connections not by the variable x, but by the rate of its change y. In

this case, for two coupled oscillators (2) , the mathematical model will have the form

$$\begin{aligned}
\frac{dx_1}{d\tau} &= y_1, \quad \frac{dy_1}{d\tau} = z_1, \\
\mu_1 \frac{dz_1}{d\tau} &= \gamma_1 - x_1 - y_1 - \varepsilon_1 z_1 - \Phi_1(x_1) - \kappa_2 \Phi_2(y_1 - y_2), \\
\frac{dx_2}{d\tau} &= y_2, \quad \frac{dy_2}{d\tau} = z_2, \\
\mu_2 \frac{dz_2}{d\tau} &= \gamma_2 - x_2 - y_2 - \varepsilon_2 z_2 - \Phi_1(x_2) - \kappa_1 \Phi_2(y_2 - y_1).
\end{aligned} \tag{5}$$

The results of the numerical experiment with the model (5) are presented in Fig. 12. Based on these results, it can be concluded that the connection of the oscillators (2) along the y coordinate makes it possible to achieve good synchronization accuracy of the simulated economic fluctuations in the ensemble. Nevertheless, this type of connection for real economic oscillators seems unrealistic, since measuring the rates of y changes in economic variables x for controlling oscillators is most likely unlikely or practically impossible.

Conclusion

The problem of synchronization of an ensemble of connected chaotic economic oscillators is considered. The economic oscillator model is an endogenous dynamic model based on the ideas of the theory of automatic control systems. Of course, this kind of general dynamic models cannot be used to obtain any specific economic estimates or specific recommendations for making economic decisions. solutions. However, such models are useful for the development of dynamic theories of economic cycles, theories of their generation, interaction, synchronization, etc., Numerical experiments with the model considered in this paper have demonstrated the qualitative similarity of chaotic oscillations generated by the model with real economic fluctuations presented in the literature. It is established that a small ensemble of related economic oscillators demonstrate the appearance of synchronization of chaotic oscillations when certain values of the coupling coefficients are reached. The synchronization of chaotic oscillations obtained in numerical experiments is characterized by the presence of a noticeable synchronization error, the magnitude of which significantly depends on the strength of the connections between the oscillators.

References

1. Samuelson P, Nordhaus W. Economics. 15th edition. New York: McGraw Hill; 1995. 792 p.
2. Vechkanov GS, Vechkanova GR. Macroeconomics. Saint Petersburg: Piter; 2002. 412 p. (in Russian).
3. Kuznetsov YA. Mathematical modeling of economic cycles: facts, concepts, results. Economic Analysis: Theory and Practice. 2011;10(17(224)):50–61 (in Russian).
4. Kuznetsov YA. Mathematical modeling of economic cycles: facts, concepts, results (end). Economic Analysis: Theory and Practice. 2011;10(18(225)):42–56 (in Russian).
5. Lebedeva AS. The genesis of the economic cycle theory. International Research Journal. 2013;8–3(15):31–34 (in Russian).
6. Lopes AM, Machado JAT, Huffstot JS, Mata ME. Dynamical analysis of the global business-cycle synchronization. PLoS ONE. 2018;13(2):e0191491. DOI: 10.1371/journal.pone.0191491.
7. Oman W. The synchronization of business cycles and financial cycles in Euro area. International Journal of Central Banking. 2019;15(1):327–362.

8. Guegan D. Chaos in economics and finance. Annual Reviews in Control. 2009;33(1):89–93. DOI: 10.1016/j.arcontrol.2009.01.002.
9. Volos C, Kyprianidis I, Stouboulos IN. Synchronization phenomena in coupled nonlinear systems applied in economic cycles. WSEAS Transactions on Systems. 2012;11(12):681.
10. Matrosov VV, Shalfeev VD. Simulation of business and financial cycles: Self-oscillation and synchronization. Izvestiya VUZ. Applied Nonlinear Dynamics. 2021;29(4):515–537 (in Russian). DOI: 10.18500/0869-6632-2021-29-4-515-537.
11. Matrosov VV, Shalfeev VD. Simulation of the business-cycle synchronization processes in an ensemble of coupled economic oscillators. Radiophysics and Quantum Electronics. 2022;64(10):750–759. DOI: 10.1007/s11141-022-10176-1.
12. McCullen NJ, Ivanchenko MV, Shalfeev VD, Gale WF. A dynamical model of decision-making behavior in a network of consumers with applications to energy choices. International Journal of Bifurcation and Chaos. 2011;21(9):2467–2480. DOI: 10.1142/S0218127411030076.
13. Ponomarenko VP. Modeling the evolution of dynamic modes in an oscillator system with frequency control. Izvestiya VUZ. Applied Nonlinear Dynamics. 1997;7(5):44–55 (in Russian).
14. Ponomarenko VV, Zaulin IA. The dynamics of an oscillator controlled by a frequency-locked loop with an inverted discriminator characteristic. J . Commun. Technol. Electron. 1997;42(7):828–835 (in Russian).
15. Kasatkin DV, Matrosov VV. Chaotic oscillations of two cascade-coupled oscillators with frequency control. Tech. Phys. Lett. 2006;32(4):357–360. DOI: 10.1134/S1063785006040250.
16. Andronov AA, Vitt AA, Khaikin SE. Theory of Oscillators. New York: Dover Publications; 1987. 815 p.
17. Belyakov LA. About structure of bifurcation multitudes in systems with separatrix loop of saddle-focus. In: Abstracts of the IX International Conference on Nonlinear Oscillations. Kiev: Institute of Mechanics of the Academy of Sciences of the Ukrainian SSR; 1981. P. 57 (in Russian).
18. Schüler YS, Hiebert P, Peltonen TA. Characterising the financial cycle: a multivariate and time-varying approach. ECB Working Paper Series. No. 1846. Frankfurt am Main: European Central Bank; 2015. 54 p. DOI: 10.2139/ssrn.2664126.
19. Shalfeev VD, Matrosov VV. Nonlinear Dynamics of Phase Synchronization Systems. Nizhny Novgorod: Nizhny Novgorod University Press; 2013. 366 p. (in Russian).